Numerical Study on RC Multilayer Perforation with Application to GA-BP Neural Network Investigation

Weiwei Sun [a], Ze Shi [b], Bingcheng Chen [a], Jun Feng [c*]

[a] Department of Civil Engineering, Nanjing University of Science and Technology, Nanjing 210094, China.

[b] State Key Laboratory of Explosion Science and Technology, Beijing Institute of Technology, Beijing 100081, China.

[c] National Key Laboratory of Transient Physics, Nanjing University of Science and Technology, Nanjing 210094, China.

Abstract

The finite element model of projectile penetrating multi-layered reinforced concrete target was established via LS-DYNA solver. The penetration model was validated with the test data in terms of residual velocity and deflection angle. Parametric analyses were carried out through the verified penetration model. Seven influential factors for penetration conditions, including the initial velocity of projectile, initial angle of attack of projectile, initial dip angle of projectile, the first layer thickness of concrete target, the residual layer thickness of concrete target, target distance and the layer number of concrete target, were put emphasis on further analysis. Furthermore, the influence of foregoing factors on residual velocity and deflection angle of projectile were numerically obtained and discussed. Based on genetic algorithm, the BP neural network model was trained by 263 sets of data obtained from the parametric analyses, whereby the prediction models of residual velocity and attitude angle of projectile under different penetration conditions were achieved. The error between the prediction data obtained by this model and the reserved 13 sets of test data is found to be negligible.

Keywords: Multi-layered Concrete Plates; Oblique Penetration; Deflection Angle; Neural Network Model.

1. Introduction

Since the Kosovo and Iraq wars, precision-guided ground-drilling weapons represented by the US Army's 'Jedam' ground-drilling missiles have developed rapidly. Researches on the damage of underground multi-story fortifications need to explore the deep mechanism of the penetration and perforation into multi-layer reinforced concrete targets [1-3]. The better understanding over projectile perforation into multi-layer RC panels may contribute to the design and construction of high-performance shelter.

At present, there is still a lack of research on multi-parameter systems for the problem of missiles penetrating multilayer reinforced concrete targets. Yue et al. [4] established a numerical calculation model of steel bullets penetrating multilayer spacer targets, and obtained the influence of the geometry, density, and mass of steel bullets on the penetration response of 5-layer spacer targets. Ji et al. [5] carried out numerical calculations on the projectile penetrating three layers of homogeneous steel plates, and obtained the velocity and acceleration change curves of the projectile, and simulated the residual velocity of the projectile perforating the three-layer target plate. Liu and Huang carried out LS-DYNA simulation research on the basis of the experiments of the projectile penetrating the three-layer

concrete target board, and obtained a reasonable numerical calculation model [6]. Sun et al. simulated the inclination of the projectile penetrating the three-layer concrete target board, obtained the time-history change curve of the projectile velocity and acceleration, and summarized the change law [7]. Yossifon et al. studied the problem of rigid body penetrating a double-layer metal target from two aspects: theoretical analysis and simulation. It was pointed out that the theoretical analysis model can significantly save computing time compared with simulation (Autodyn2D) [8]. Booker et al. compared the penetration effects of 6 groups of equal-volume segmented concrete and monolithic concrete, showing that under the same anti-penetration effect, a method can be found to segment large monolithic concrete target into segmented concrete plates, to reduce the cost of the protective structures [9].

In this work, a finite element model of the projectile penetrating the multilayer reinforced concrete target is established with validation against the test results. Extensive simulations are conducted to analyze 7 penetration factors, such as initial velocity (v_0), initial inclination (θ_0), initial angle of attack (δ), first-layer target thickness (t_1), remaining Target thickness (t_2), target distance (s), number of target layers (n), etc. on the projectile's remaining velocity (v_r) and deflection angle (α). Using the genetic algorithm's BP (GA-BP) neural network model for the parametric analysis results to perform machine learning training, the prediction models of the missile's residual velocity and attitude angle under different penetration conditions can be developed. The GA-BP neural network predictions agree well with the foregoing numerical modeling results.

2. Finite Element Model and Verification of Steel-multilayer Target Penetration

2.1. Introduction to Verification Test Background

The test results of the projectile penetrating the multilayer concrete target in [10] were used to verify the simulation results. The test projectile material is high-strength steel 30CrMnSiA, the projectile length is 1200 mm, the mass is 290 kg, the projectile head coefficient CRH = 3.0, and the center of gravity is 637 mm from the head. The thickness of the first layer of concrete target is 300 mm, and the thickness of the remaining targets is 180 mm. The length and width of each layer of the target plate are 4000 mm. The vertical distance between adjacent target plates is 3.5m, and the angle between the target plate and the ground normal is 17°. The uniaxial compressive strength for concrete is 40 MPa and the volume reinforcement ratio is 0.3%. The projectile was fired horizontally with an initial velocity of 688 m/s.

Table 1. Concrete and rebar material parameters

Concrete				Rebar	
Density (ρ)/kg•m^{-3}	2525	Normalized maximum intensity (S_{max})	7	Density (ρ)/kg•m-3	7800
Shear modulus (G)/GPa	8.76	Crushing pressure (P_{crush})/GPa	0.016	Elastic Modulus (E)/GPa	200
Normalized cohesive strength (A)	0.79	Crushing volume strain (μ_{crush})	0.001	Poisson's ratio (v)	0.3
Normalized pressure hardening coefficient (B)	1.6	Compaction pressure (P_{lock})/GPa	0.81	Yield Strength (f_y)/GPa	0.335
Strain rate coefficient (C)	0.007	Compacted volume strain (μ_{lock})	0.1	Hardening parameters (β)	0
Strain hardening index (N)	0.61	Damage constant (D_1)	0.04	Strain rate influence factor (n)	40
Quasi-static uniaxial compressive strength (f_c)/GPa	0.04	Damage constant (D_2)	1	Strain rate influence factor (m)	5
Hydrostatic pressure (T)/GPa	0.004	Pressure constant (K_1)/GPa	85	Tangent modulus (E_{tan})/GPa	1
Reference strain rate (ε_c)	-1	Pressure constant (K_2)/GPa	-171	Failure strain	0.12
Minimum plastic strain before fracture (ε_{min})	0.01	Pressure constant (K_3)/GPa	208		

2.2. Establishment of Finite Element Model

In this paper, a finite element model of the projectile penetrating the multilayer reinforced concrete target is established via the LS-DYNA software. In the finite element model, the element type of the reinforcing bar is BEAM161, and the target plates are modeled with SOLID 164. Since the projectile has almost no deformation after penetration test [10-11], the projectile in simulation can be regarded as a rigid body. Considering the projectile's own weight, a weight load was applied to the body. The material model of the steel bar is MAT_PLASTIC_KINEMATIC, and the material model of the concrete is MAT_JOHNSON_HOLMQUIST_CONCRETE (referred to as HJC [12]). See Table 1 for specific material model parameters.

2.3. Comparative Analysis of Numerical Calculation Results and Experimental Results

Figure 1 is a comparison diagram of penetration snapshots as a projectile penetrates a four-layer target plate, taken by a high-speed photography device in the test, and penetration figures of a numerical calculation model.
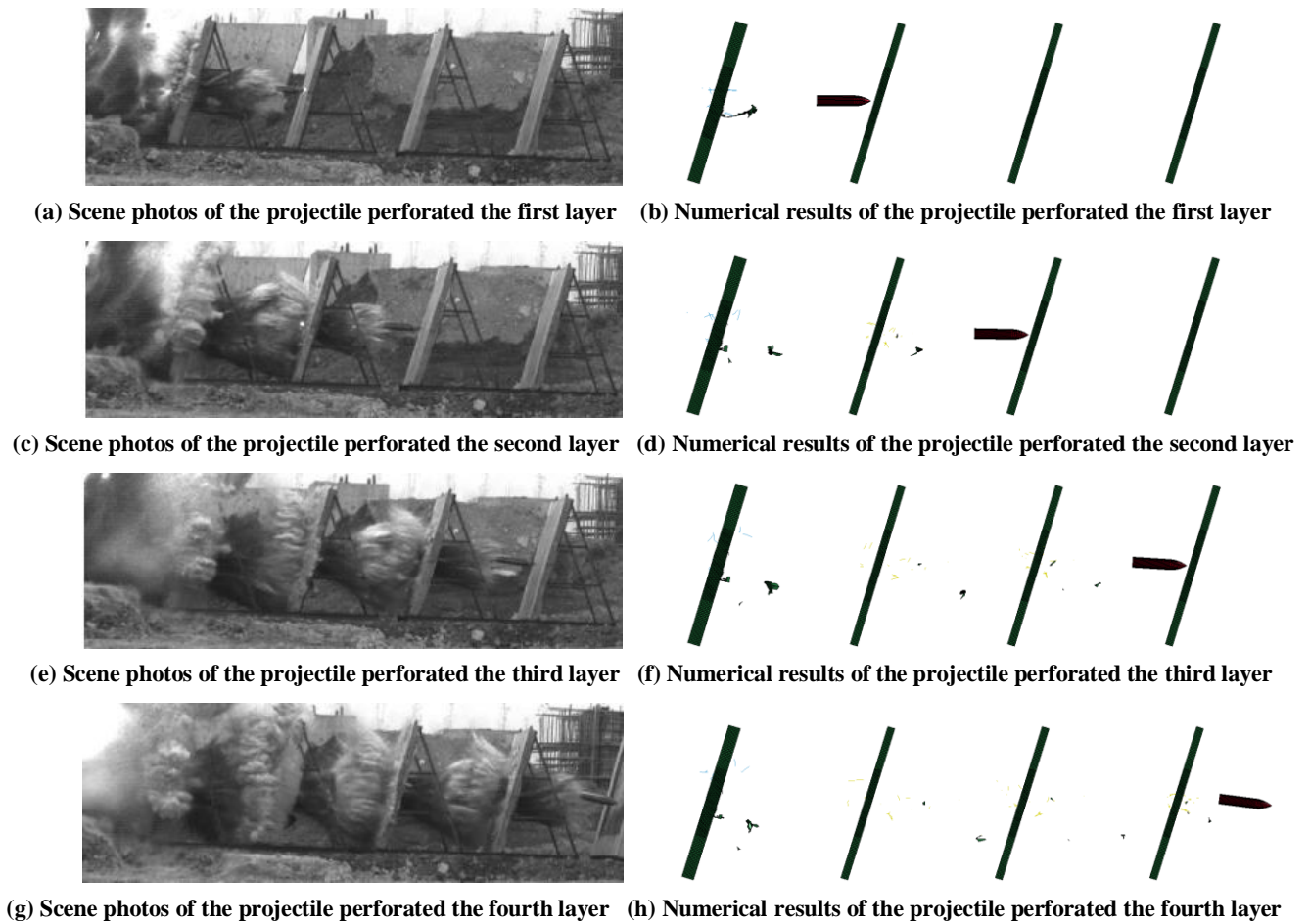
(a) Scene photos of the projectile perforated the first layer   **(b) Numerical results of the projectile perforated the first layer**

(c) Scene photos of the projectile perforated the second layer   **(d) Numerical results of the projectile perforated the second layer**

(e) Scene photos of the projectile perforated the third layer   **(f) Numerical results of the projectile perforated the third layer**

(g) Scene photos of the projectile perforated the fourth layer   **(h) Numerical results of the projectile perforated the fourth layer**

Figure 1. Comparison of field photos and numerical results of the projectile penetrating the four-layer plates

It can be observed from Figure 1 (a)-(h) that the finite element model can simulate the whole process of the elastic body penetrating the four-layer reinforced concrete target. The horizontal (x-axis) residual velocity v_r and the deflection angle α for projectile for perforating each target plate layer can be obtained through simulation results. The comparison between simulation and test data is shown in Figure 2. The experimental data are in good agreement with the simulation results, ensuring that the simulation model in this paper can be used to study the parameters of the projectile penetrating the multilayer reinforced concrete target. The attitude deflection in a medium concrete target is under the deflection mechanisms of both the initial cratering and the shear plugging sub-stages as well as the incomplete clamping mechanism of the tunneling sub-stage. In brief, Duan et al. [13] gave the explanation to the deflection mechanism claiming that the projectile tends to perforate the concrete panel in the shortest path.
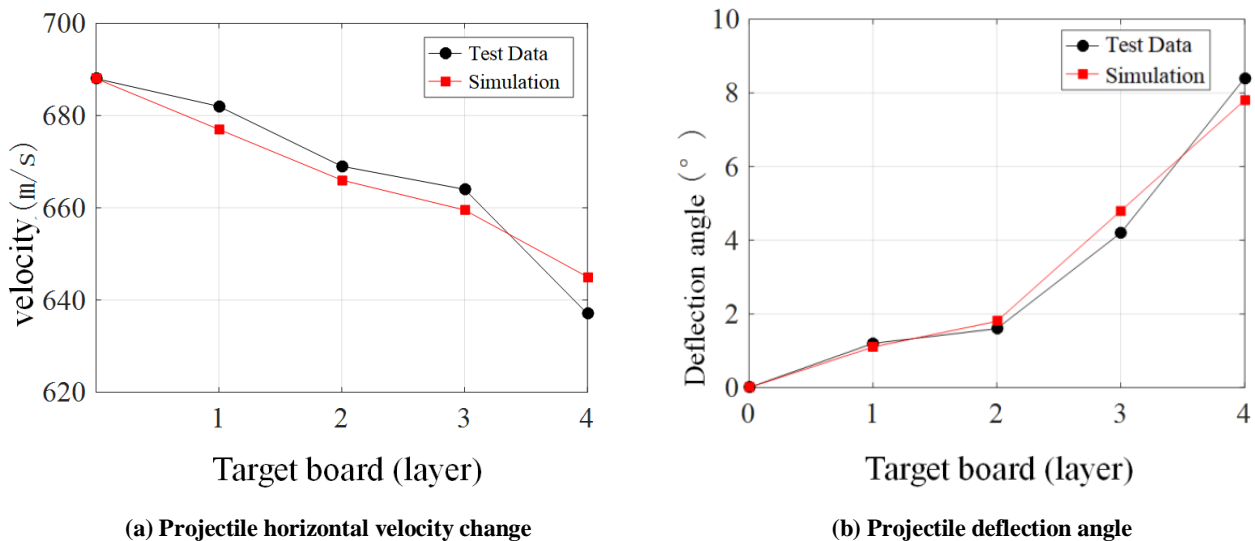
(a) Projectile horizontal velocity change   **(b) Projectile deflection angle**

Figure 2. Comparison of simulation and test results

(a) *t* = 2.75 ms

(b) *t* = 5.99 ms

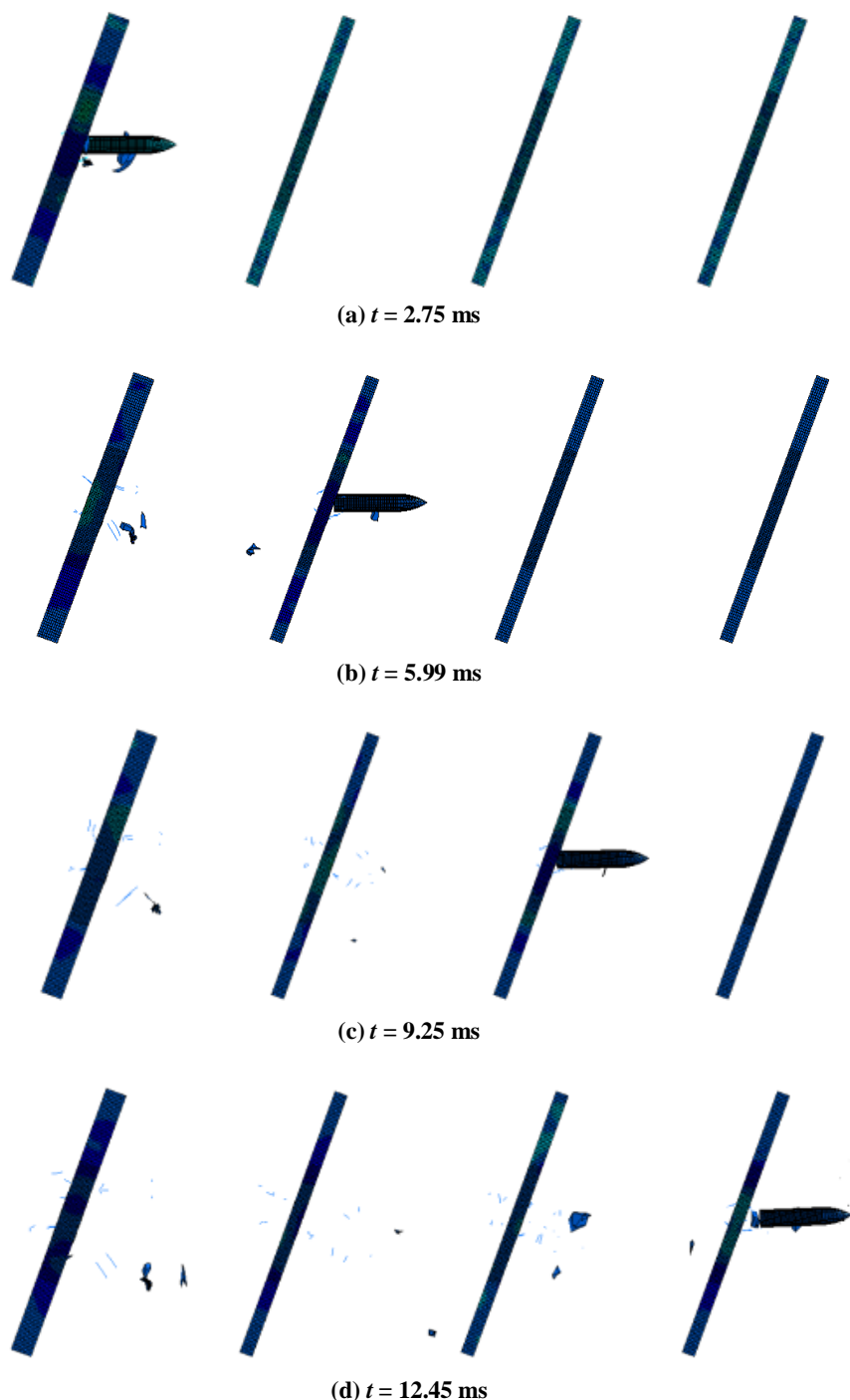**(c)** *t* = 9.25 ms

(d) *t* = 12.45 ms

Figure 3. Penetration of 20° inclination projectile

3. Analysis of Factors on Penetration in Multi-layer Steel Target

3.1. Projectile Penetrating into Multilayer Target

Figure 3 shows the whole process of the projectile penetrating the reinforced concrete four-layer target board in the finite element model. Different from the test state in [10], it is a state where the actual simulated missile body invades the target from the top, and the direction of gravity is adjusted to the horizontal direction. The basic parameters are set as follows: the initial velocity of the projectile is $v_0 = 1000$ m/s, and the angle of attack is 0°; the thickness of the first layer of concrete target is 300 mm, and the 3 other plates' thickness is 180 mm. The angle (θ_0) between the target plate and the YZ plane is 20°. The concrete and reinforcement parameters are the same as those in Table 1.
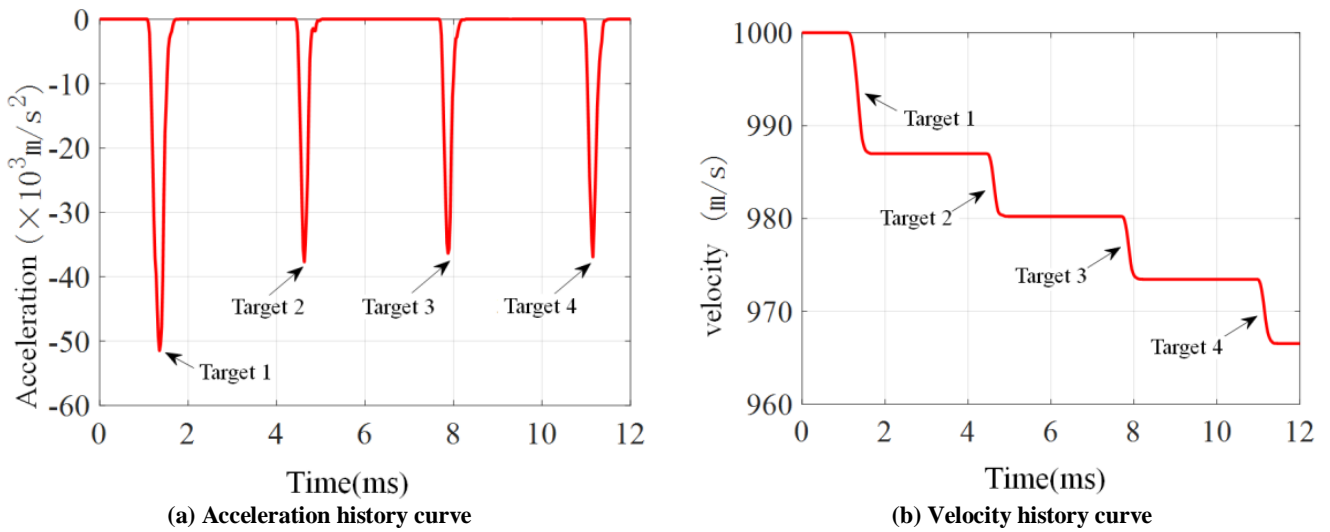
(a) Acceleration history curve

(b) Velocity history curve

Figure 4. Changes in projectile velocity and acceleration at 20° inclination

(a)Target 1   (b)Target 2

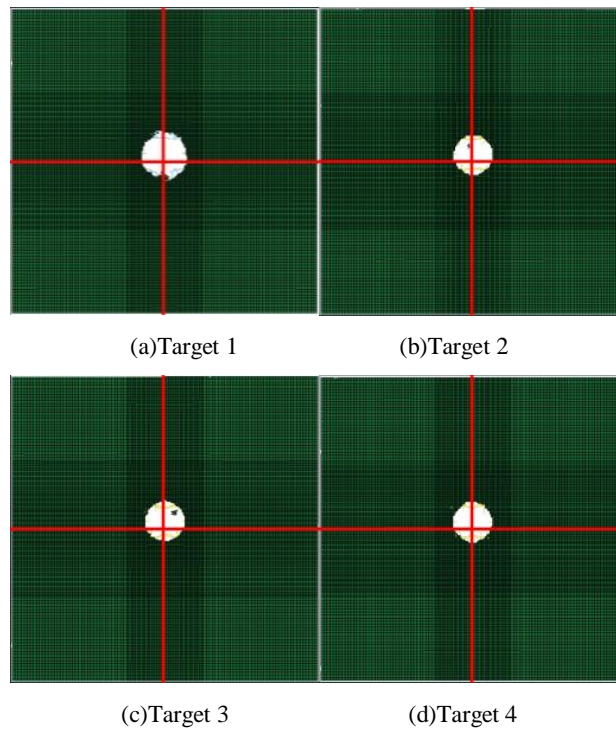(c)Target 3   (d)Target 4

Figure 5. The damage of the target plates no. 1 to 4 subjected to projectile with 20° inclination

According to Figure 3, the deflection angle of the projectile during the penetration of the first layer of the target board is 0.16°, and the residual velocity of the projectile in the x-axis direction is 987.0 m/s. As the projectile passes through the fourth layer of the target board, the body deflection angle is enlarged to 1.23°, and the residual velocity of the projectile is 966.52 m/s.

The time-history curve of the projectile acceleration in Figure 4 (a) shows that the first-layer target has greatest resistance to the projectile, while the subsequent three-layer thin-target resistance peaks tend to be lower but consistent. This is because after the penetration speed is reduced, the ratio of the static resistance item becomes larger, and the penetration resistance is less affected by the reducing projectile velocity. From Figure 5, it reveals that the ballistic tunnel is approximately a circle, and the diameter of the tunnel of the first-layer target plate is slightly larger than that of the other 3 layers. For the sake of visualization, an auxiliary cross cursor at the initial impact point [14]. From the position relationship between the initial impact point of the projectile and the damage opening of each layer of target plate is added, it can be seen the projectile trajectory has a tendency to gradually shift upward.

3.2. Effect of Inclination

The initial horizontal velocity of the projectile is 1000 m/s, and the angle of attack is 0°. Since ricochet are liable to happen if the oblique angle and yaw are too large to neglect [15]. The initial inclination angles $\theta_0 = 10°$, 15°, 20°, 25°, and 30° are selected for parametric analysis.

Figure 6 shows the change of the deflection angle of the projectile after passing through the target plate at different initial inclination angles. When the inclination angle is 10-20°, the deflection angle of the projectile is very small, and the maximum deflection angle is only 1.23°. In terms of difference, the difference between the deflection angles between different tilt angles is within 1°. When the initial inclination of the projectile is 25-30°, the deflection angle of the projectile during the penetration process is significantly enlarged, and the deflection angle of each layer is more than 60% larger than the previous layer, and the maximum deflection angle reaches 6.2°.

Figure 7 shows the velocity change of the projectile at different inclination angles. When the same inclination angle penetrates through four layers of reinforced concrete target plates, the speed in the x-axis direction changes almost linearly, and the speed decreases by approximately 7% after passing through each layer of target plates. There is little difference in the speed of the x-axis direction between different inclination angles. The difference between the final residual velocity of the inclination angle of 10° and the inclination angle of 30° is only 4.3 m/s, i.e., effect of the inclination angle on the speed drop is not very obvious.
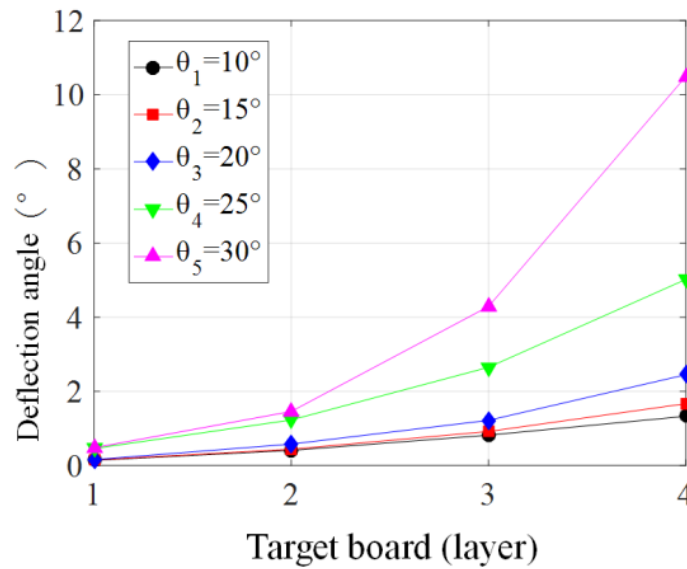

Figure 6. Deflection angle of the lower projectile at different inclination angles
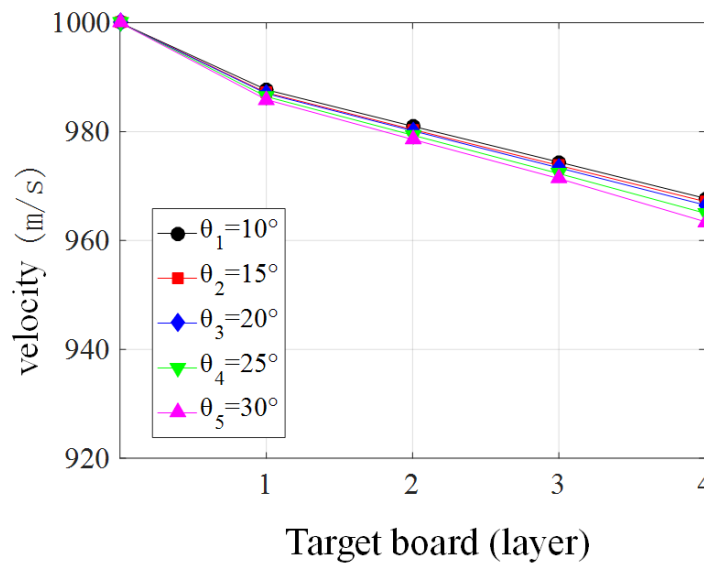

Figure 7. Residual velocity of the projectile at different inclination angles

3.3. Effect of Attack Angle

Under 1000 m/s initial horizontal velocity and no inclination angle, the initial attack angles δ = 1°, 2°, 3°, 4°, and 5° are selected for parameter analyses.
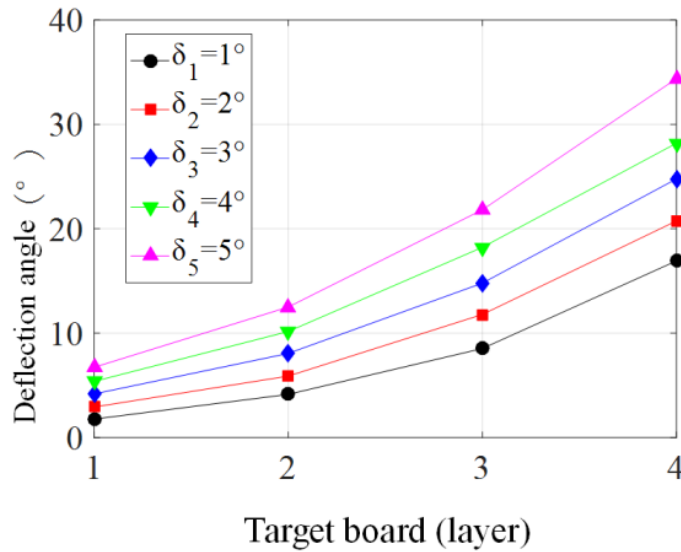

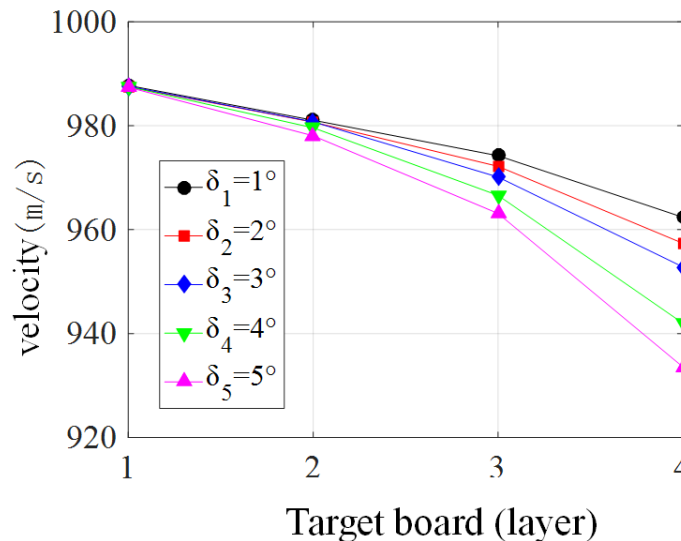**Figure 8. Deflection angle of the projectile at different angles of attack**

Figure 9. Residual velocity of the projectile under different attack angles

It can be observed from Figure 8 that the angle of attack has a great influence on the deflection angle of the projectile penetration. When the initial angle of attack is only 1°, the projectile still produce a large deflection. When penetrating the same layer of target plate, each time the initial angle of attack increases by 1° leading to 20% increase of projectile deflection angle.

Figure 9 suggests that as the projectile penetrates the first two layers of targets, the difference in the residual velocity of the projectile in the x-axis direction is very small whereby the maximum residual velocity difference is only 3 m/s. According to the reduction of the velocity of the projectile in the x-axis direction, the penetration attack angle can be divided into two ranges: 1-3° and 3-5°. Penetrating the same concrete target plates, the projectile velocity decreases linearly for 1-3°attack angle range, meanwhile the velocity drops more dramatically for 3-5° attack angle.

3.4. Effect of Initial Velocity, Target Thickness, and Target Distance

It is important to have a comprehensive understanding of the missile penetrating the multilayer target taking more parameters into account. Considering the effect of the angle of attack on the penetration of the multilayer target by the missile, it is necessary to study the following three factors of the initial velocity of the missile: the thickness of the target, and the distance between the targets.

3.4.1. Effect of Initial Velocity

With 1° initial projectile attack angle and no inclination angle, the initial velocity $v_0 = 600, 800, 1000$ and 1200 m/s are selected for simulation. It is observed from Figure 10, the smaller initial velocity causes greater projectile deflection angle. For larger initial velocity case, the projectile velocity decreases more dramatically after passing through the target plates, as shown in Figure 11. This is because the penetration resistance is significantly greater when penetration velocity is large [16].
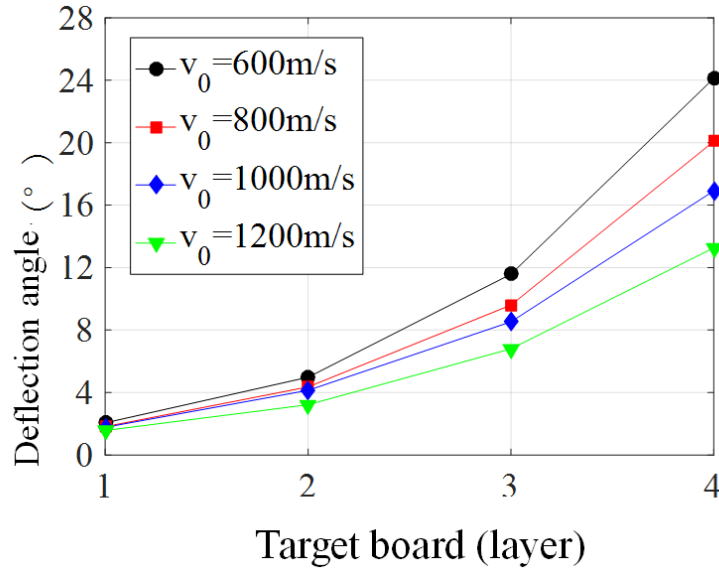

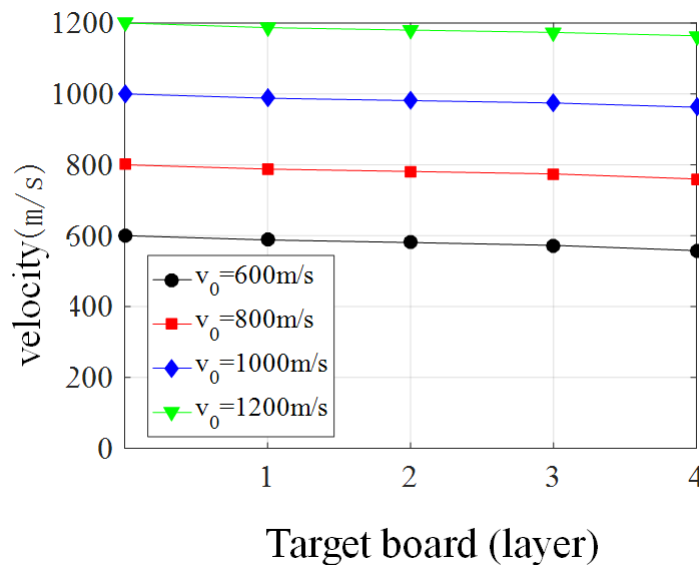**Figure 10. Deflection angle of the projectile at different initial speeds**

Figure 11. Residual velocity of the projectile under different initial velocity penetration

3.4.2. Effect of Target Thickness

With 1° initial attack angle and no inclination angle, the initial velocity with 1000 m/s is studied herein. The thickness of the first layer target plate $t_1 = 200$ mm, 300 mm, 400 mm (corresponding to the target thickness $t_2 = 120$ mm, 180 mm, 240 mm) are numerically investigated.

It can be seen from Figure 12 that the deflection angle of the projectile increases with the thickness of the target plate. For the same layer of target plate, the deflection angle of the projectile through the 300 mm thickness target plate is about 2 to 2.5 times the thickness of 200 mm. For the same layer, the deflection angle of the projectile through the 400 mm thickness target plate is about 300 mm. It can be seen from Figure 13 that when the bullet penetrates the first three layers of the target plate, the velocity in the x-axis direction changes linearly, and when it penetrates the fourth layer, the speed significantly decreases.
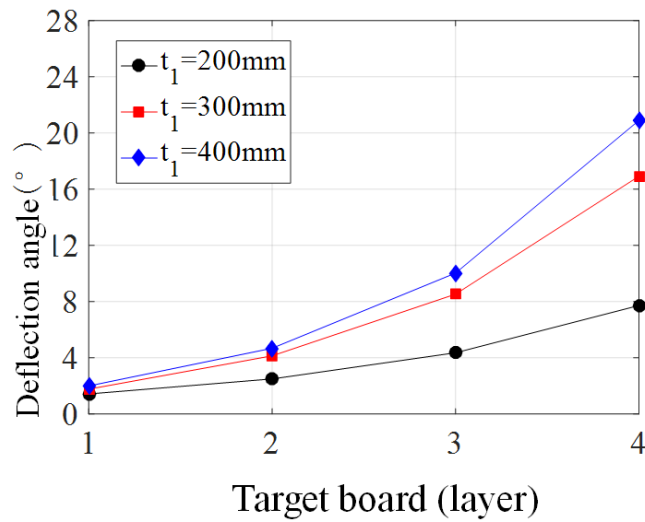
Figure 12. Deflection angle of the projectile with different target thickness
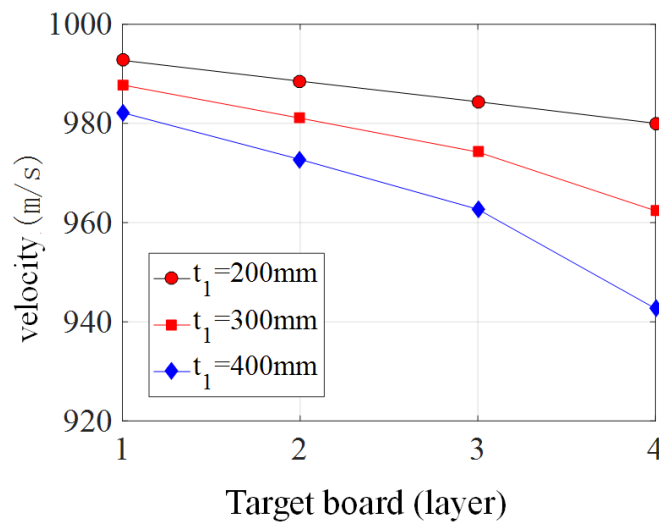

Figure 13. Residual velocity of the projectile with different target thickness

3.4.3. Effect of Initial Velocity

With 1° initial attack angle, 0 inclination angle and 1000 m/s initial velocity, and the target plate spacing s = 2000 mm, 3000 mm, 4000 mm is selected for simulation.
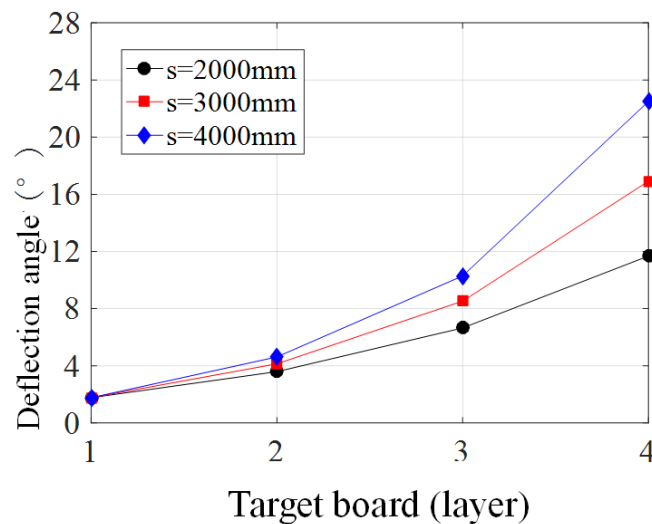

Figure 14. Variation of attitude angle at different target plate spacing
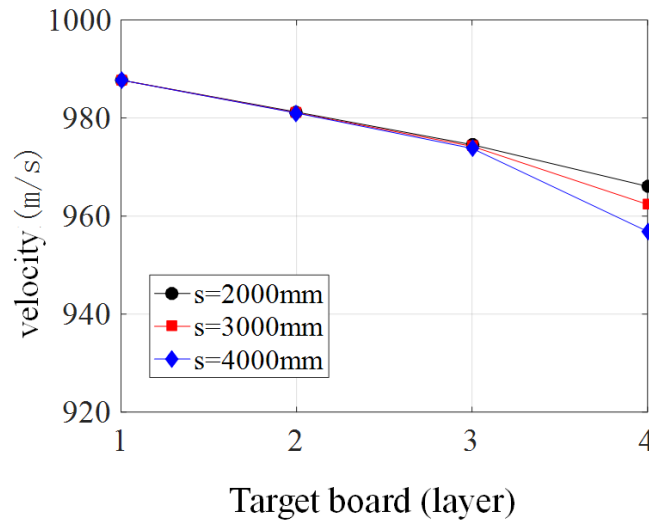
Figure 15. Residual velocity at different target plate spacing

It can be seen from Figure 14 that the deflection angle of the projectile increases with the increase of the target plate spacing. For the same target plate spacing, the deflection angle of this layer is about twice that of the previous layer. As for the target plate, there is a linear growth relationship between the projectile deflection angle and the target distance. It can be seen from Figure 15 that under 1° attack angle, the speed change in the x-axis direction is roughly linear when the target plate spacing is between 2000 mm and 4000 mm. As the projectile penetrates the fourth-layer target board, the speed change no longer conforms to the previous linear relationship, and the speed decreases even more dramatically.
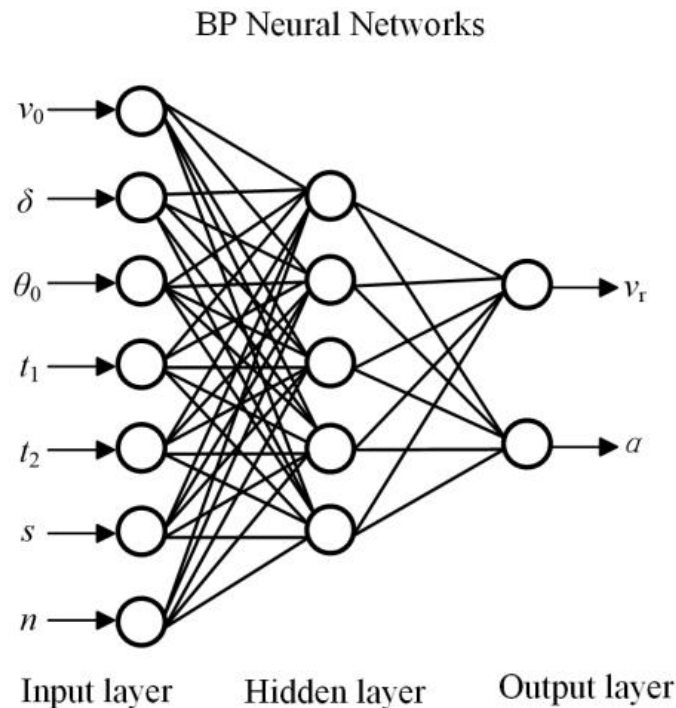
Figure 16. BP neural network model principle diagram

4. Establishment of GA-BP Neural Network Prediction Model

Artificial neural network is a kind of intelligent algorithm that is established by memorizing and processing information on the neural network of the brain. The BP algorithm is a multi-layer learning error back propagation algorithm, and the genetic algorithm introduces the genetic and evolutionary mechanisms of the biological world into the process of simulation calculation, and randomly searches for the global optimal solution by simulating the process of natural evolution. In recent years, BP neural network models based on genetic algorithms have been widely used in the field of nonlinear problem prediction [17-19].

4.1. Neural Network Model Design

The BP neural network model is established based on MATLAB software which structure is shown in Figure 16 [20]. Seven neural units are set in the first layer (input layer) to correspond to the seven penetration impact factors to be considered in training: the initial velocity of the projectile (v_0), initial angle of attack (δ), initial angle of inclination (θ_0), target thickness of the first layer (t_1), remaining target thickness (t_2), target distance (s), number of target layers (n); at the output layer of the network There are two neural units: the horizontal velocity of the projectile (v_r) and the deflection angle (α). In the model, the transfer function of the second layer (hidden layer) is selected as the tansig function. It uses its own saturated nonlinearity and differentiability to enhance the ability of network model nonlinear mapping. The transfer function of the third layer (output layer) is selected as the 'purelin' function, which can make the output value of the network any value.

4.2. Definition of Initialization Parameters

(1) Selection of initial weight and threshold

For a general BP neural network, the initial weights and thresholds are randomly selected in the interval (-1, 1). This paper uses genetic algorithm to optimize the BP neural network [18, 21]. The initial population is defined as 50, the number of evolutions is 100, the crossover probability is 0.8, and the mutation probability is 0.09.The optimal individual obtained is decoded as the initial weight and threshold of the BP neural network.

(2) Selection of learning rate

The size of the learning rate can directly determine the magnitude of the weight changes that the network model generates in each training. Too much learning efficiency will cause network instability and even network paralysis. The lower learning efficiency will make the convergence speed of the network model during training very slow. Generally speaking, the value of learning efficiency is between 0.01-0.8, and the learning rate is chosen as 0.01 in this paper.

(3) Selection of expected error

The training stops when the error value of the network training reaches the specified limit. When the value of the expected error is too small, it is difficult to reach the standard during the network training process, and even "overfitting" may occur. When the value of the expected error is too large, the accuracy of the network model is difficult to meet the actual needs. In this work, the expected error is 0.0001.

(4) Selection of training steps

A larger number of training steps can make the training more accurate. Improper parameter setting and an increase in the number of training steps can only cause the network training model to diverge. On the premise that the above models and parameters have been determined, the maximum number of training steps is finally determined to be 10,000, and the output is defined to be displayed every 50 steps.

4.3. Selection and Processing of Training Samples

The quality of the neural network model and the strength of its prediction ability are based on the training of a large amount of accurate data, so the selection of accurate and reliable training sample data is crucial for the establishment of the neural network. The 263 sets of data obtained from the parameter analysis were extracted and divided into two groups, one of which was 250 data for training the established GA-BP neural network model, and the other was 13 data as a pair Detection of network model accuracy. The variation range of the training data of the neural network is as follows: (1) initial tilt angle (θ_0=10°, 15°, 20°, 25°, 30°); (2) initial angle of attack (δ=1°, 2°, 3°, 4°, 5°); (3) Initial speed (v_0= 600, 800, 1000, 1200 m/s); (4) First layer target thickness (t_1= 200, 300, 400 mm); (5) remaining target thickness (t_2=120, 180, 240 mm); (6) target distance (s= 2000, 3000, 4000 mm); (7) number of layers (n=1, 2, 3, 4).

The data samples used for network testing are shown in Table 2. The 13 sets of data are not included in the training data samples, thereby ensuring that the network model has reliable accuracy.

4.4. GA-BP Neural Network Prediction and Result Analysis

Call the sim function to predict the reserved test data samples. The predicted values calculated by the network are compared with the actual test output values. The specific values are shown in Table 3. The result of comparison shows that the residual velocity error is within 5%, and the attitude angle of the projectile does not exceed 11.2%. It can be considered that the GA-BP neural network model trained in this paper is suitable for the prediction of the projectile penetrating the multilayer concrete target. It worth noting that the combined influence of initial inclination and attack angles is larger than a single factor since more complicated loading is acting on the projectile body. Moreover, it

reveals that the combined effect of initial inclination and attack angles may neutralize the defection effect. This phenomenon has been observed by Gao and Li [22, 23] which declares that a proper negative attack angle which can minimize the trajectory turning in oblique penetration cases.

Table 2. Sample test data of the network model

Number	v_0 (m/s)	δ (°)	t_1 (mm)	t_2 (mm)	s (mm)	θ_0 (°)	n	v_r (m/s)	α (°)
1	1000	0	300	180	3000	10	1	987.7	0.14
2	1000	0	300	180	3000	20	4	966.52	2.45
3	1000	0	300	180	3000	30	4	963.46	10.49
4	1000	2	300	180	3000	0	4	957.36	20.75
5	1000	4	300	180	3000	0	3	966.59	18.22
6	1000	5	300	180	3000	0	4	933.57	34.37
7	600	1	300	180	3000	0	3	572.68	11.58
8	1200	1	300	180	3000	0	4	1162.36	13.27
9	1000	1	400	240	3000	0	2	972.73	4.68
10	1000	1	300	180	2000	0	3	974.56	6.65
11	1000	1	300	180	3000	20	1	986.98	1.8
12	1000	2	300	180	3000	20	2	979.67	6.97
13	1000	3	300	180	3000	20	4	943.24	31.53

Table 3. Comparison of network predictions and test values

Number	v_r (m/s)			α (°)		
	Forecast data	Test Data	Error (%)	Forecast data	Test Data	Error (%)
1	987	987.7	-0.07	0.15	0.14	6.25
2	964.3	966.52	-0.22	2.7	2.45	10.2
3	964.1	963.46	0.06	9.8	10.49	-6.57
4	956.3	957.36	-0.11	21.2	20.75	2.16
5	968.3	966.59	0.17	17.6	18.22	-3.4
6	937.6	933.57	0.43	33.5	34.37	-2.53
7	571.8	572.68	-0.15	11.3	11.58	-2.41
8	1162.2	1162.36	-0.01	13.4	13.27	0.97
9	973.2	972.73	0.048	4.4	4.68	-5.98
10	974.5	974.56	-0.006	6.7	6.65	0.75
11	986.1	986.98	-0.08	1.6	1.8	-11.11
12	979.4	979.67	-0.02	6.9	6.97	-1
13	941.2	943.24	-0.21	32	31.53	1.49

5. Conclusions

Based on the LS-DYNA numerical simulation software, a finite element model for the projectile penetrating the reinforced concrete multilayer target is established, and the model results are verified with experiments. 7 penetration factors: including the initial velocity (v_0), initial angle of attack (δ), initial tilt angle (θ_0), target thickness of the first layer (t_1), remaining target thickness (t_2), target distance (s), and number of target layers (n) are investigated to analyze their effects on the projectile residual velocity (v_r) and deflection angle (α). Based on GA-BP neural network, a prediction model of projectile penetrating reinforced concrete multilayer targets is then proposed. The main conclusions are drawn as follows:

- A single parameter angle of attack has a greater effect on the deflection angle of the projectile penetration. When the attack angle is 1°, the projectile still produces a large deflection angle. When penetrating the same layer of target plate, each time the attack angle increases by 1° while the deflection angle of the projectile increases by about 20%. With a single parameter, the projectile deflection angle is negligible when the inclination of the projectile is 10-20°. When the initial inclination of the projectile is 25-30°, the deflection

angle of the projectile during the penetration process is significantly enlarged, and the inclination angle is highly related to the velocity. The effect of projectile falling down is not obvious.

- Under 1°initial attack angle, the projectile velocity changes linearly in the x-axis direction as it passes through the first three layers of target plates under the combined influence of different parameters such as target plate thickness and target plate spacing. During penetration the fourth concrete layer, the projectile velocity decreased significantly.

- The GA-BP neural network model established in this paper has good prediction ability for residual velocity and deflection angle of the projectile penetration in reinforced concrete multilayer target plates.

6. Funding

7. Conflicts of Interest

The authors declare no conflict of interest.

8. References

[1] Feng, Jun, Meili Song, Qiang He, Weiwei Sun, Lei Wang, and Kaijing Luo. "Numerical Study on the Hard Projectile Perforation on RC Panels with LDPM." Construction and Building Materials 183 (September 2018): 58–74. doi:10.1016/j.conbuildmat.2018.06.020.

[2] Luo, Wen, Viet T. Chau, and Zdeněk P. Bažant. "Effect of High-Rate Dynamic Comminution on Penetration of Projectiles of Various Velocities and Impact Angles into Concrete." International Journal of Fracture 216, no. 2 (March 5, 2019): 211–221. doi:10.1007/s10704-019-00354-0.

[3] Ma Zhaofang, Zhuoping Duan, Zhuocheng Ou, and Fenglei Huang. Experimental and numerical simulation of projectile obliquely penetrating multilayer spaced concrete targets [J]. Journal of Beijing Institute of Technology 36 (10) (2016): 1001-1005. doi:10.15918/j.tbit1001-0645.2016.10.003.

[4] Yue Xiaobing, Yuan Long, Xiang Fang and Wen Xie. Simulation of high-speed simulation of steel projectile penetrating multilayer targets [J]. Journal of PLA University of Science and Technology, Natural Science Edition 4 (4) (2003): 40-44. doi:10.3969/j.issn.1009-3443.2003.04.010.

[5] Ji Xia, Li Wang. Numerical analysis of projectile penetrating multilayer target [J]. Journal of Detection and Control, 2006, 28 (2): 42-45.

[6] Haipeng Liu, Shiqiao Gao, Lei Jin. Experimental and simulation analysis of projectile penetrating through a finite concrete target [J]. Ordnance Industry Journal, 2010 (s1): 59-63.

[7] Junwei Sun, Ya Zhang, Shizhong Li. Analysis of Overload Characteristics of Projectile Penetrating into Targets with Different Spacing [J]. Journal of North University of China (Natural Science Edition), 2013, 34 (1): 24-28.

[8] Yossifon, G., A.L. Yarin, and M.B. Rubin. "Penetration of a Rigid Projectile into a Multi-Layered Target: Theory and Numerical Computations." International Journal of Engineering Science 40, no. 12 (July 2002): 1381–1401. doi:10.1016/s0020-7225(02)00013-7.

[9] Booker, Paul M., James D. Cargile, Bruce L. Kistler, and Valeria La Saponara. "Investigation on the Response of Segmented Concrete Targets to Projectile Impacts." International Journal of Impact Engineering 36, no. 7 (July 2009): 926–939. doi:10.1016/j.ijimpeng.2008.10.006.

[10] Feng Jie. Numerical simulation of attitude deflection of projectile penetrating thin concrete target [D]. Beijing Institute of Technology, 2016.

[11] Feng, Jun, Wenjin Yao, Weixin Li, and Wenbin Li. "Lattice Discrete Particle Modeling of Plain Concrete Perforation Responses." International Journal of Impact Engineering 109 (November 2017): 39–51. doi:10.1016/j.ijimpeng.2017.05.017.

[12] Feng, Jun, Weiwei Sun, Zhilin Liu, Chong Cui, and Xiaoming Wang. "An Armour-Piercing Projectile Penetration in a Double-Layered Target of Ultra-High-Performance Fiber Reinforced Concrete and Armour Steel: Experimental and Numerical Analyses." Materials & Design 102 (July 2016): 131–141. doi:10.1016/j.matdes.2016.04.021.

[13] Duan, Zhuo-ping, Shu-rui Li, Zhao-fang Ma, Zhuo-cheng Ou, and Feng-lei Huang. "Attitude Deflection of Oblique Perforation of Concrete Targets by a Rigid Projectile." Defence Technology (September 2019). doi:10.1016/j.dt.2019.09.009.

[14] Smith, Jovanca, Gianluca Cusatis, Daniele Pelessone, Eric Landis, James O'Daniel, and James Baylot. "Discrete Modeling of Ultra-High-Performance Concrete with Application to Projectile Penetration." International Journal of Impact Engineering 65 (March 2014): 13–32. doi:10.1016/j.ijimpeng.2013.10.008.

[15] Chen, Xuguang, Fangyun Lu, and Duo Zhang. "Penetration Trajectory of Concrete Targets by Ogived Steel projectiles– Experiments and Simulations." International Journal of Impact Engineering 120 (October 2018): 202–213. doi:10.1016/j.ijimpeng.2018.06.004.

[16] Feng, Jun, Wenbin Li, Xiaoming Wang, Meili Song, Huaqing Ren, and Weibing Li. "Dynamic Spherical Cavity Expansion Analysis of Rate-Dependent Concrete Material with Scale Effect." International Journal of Impact Engineering 84 (October 2015): 24–37. doi:10.1016/j.ijimpeng.2015.05.005.

[17] Duraku, Ramadan K, and Riad Ramadani. "Development of Traffic Volume Forecasting Using Multiple Regression Analysis and Artificial Neural Network." Civil Engineering Journal 5, no. 8 (August 21, 2019): 1698–1713. doi:10.28991/cej-2019-03091364.

[18] Chi, Li, and Li Lin. "Application of BP Neural Network Based on Genetic Algorithms Optimization in Prediction of Postgraduate Entrance Examination." 2016 3rd International Conference on Information Science and Control Engineering (ICISCE) (July 2016). doi:10.1109/icisce.2016.57.

[19] Ding, Shifei, Chunyang Su, and Junzhao Yu. "An Optimizing BP Neural Network Algorithm Based on Genetic Algorithm." Artificial Intelligence Review 36, no. 2 (February 18, 2011): 153–162. doi:10.1007/s10462-011-9208-z.

[20] Adeli, Hojjat. "Neural Networks in Civil Engineering: 1989–2000." Computer-Aided Civil and Infrastructure Engineering 16, no. 2 (March 2001): 126–142. doi:10.1111/0885-9507.00219.

[21] Al-Ani, Rami Raad Ahmed, and Basim Hussein Khudair Al-Obaidi. "Prediction of Sediment Accumulation Model for Trunk Sewer Using Multiple Linear Regression and Neural Network Techniques." Civil Engineering Journal 5, no. 1 (January 27, 2019): 82. doi:10.28991/cej-2019-03091227.

[22] Gao, Xudong, and Q. M. Li. "Trajectory and Loads for Oblique Penetration Into Concrete Targets by Rigid Projectile." 31st International Symposium on Ballistics (December 2, 2019). doi:10.12783/ballistics2019/33218.

[23] Gao, Xudong, and Q. M. Li. "Effects of Structure Characteristics of Projectile on Trajectory and Loads for Oblique Penetration into Concrete." 31st International Symposium on Ballistics (December 2, 2019). doi:10.12783/ballistics2019/33220.